



# Synthesis, crystal structure, and electrical and magnetic properties of $\text{Ce}_3\text{MoO}_7$

Philippe Gall<sup>a,\*</sup>, Patrick Gougeon<sup>b</sup>

<sup>a</sup> Laboratoire de Chimie du Solide et Inorganique Moléculaire, UMR CNRS 6226, Université de Rennes 1, Avenue du Général Leclerc, 35042 Rennes cedex, France

<sup>b</sup> Laboratoire de Chimie des Matériaux Inorganiques et de Cristallographie, 20 avenue des buttes de Coesmes, 35043 Rennes cedex, France

## ARTICLE INFO

### Article history:

Received 7 January 2009

Received in revised form

23 January 2009

Accepted 30 January 2009

Available online 6 February 2009

### Keywords:

Reduced molybdenum oxides

Molybdenum chains

Rare-earths

Magnetic susceptibility

Resistivity measurement

## ABSTRACT

Powder samples and single crystals of the ternary oxide  $\text{Ce}_3\text{MoO}_7$  were obtained by solid state reaction. The structure was determined by single-crystal X-ray diffraction.  $\text{Ce}_3\text{MoO}_7$  crystallizes in the orthorhombic space group  $P2_12_12_1$  (no. 19) with unit-cell parameters  $a = 7.5395(2)\text{Å}$ ,  $b = 7.6769(1)\text{Å}$ ,  $c = 10.9769(2)\text{Å}$  and  $Z = 4$ . Full-matrix least-squares refinement on  $F^2$  using 3903 independent reflections for 101 refinable parameters results in  $R_1 = 0.0281$  and  $wR_2 = 0.0473$ . The structure consists of chains of corner-linked  $\text{MoO}_6$  octahedra running parallel to the  $b$ -axis and separated from each other by seven- or eight-coordinate Ce–O polyhedra. The trend of the unit-cell parameters of the  $\text{Ln}_3\text{MoO}_7$  series, plotted versus the  $R^{3+}$  ionic radius, shows a linear behavior, which strongly suggests a trivalent state for the Ce atoms. Magnetic susceptibility measurements confirm that the oxidation state of the Ce atoms is +3. Resistivity measurements on a single crystal show that the  $\text{Ce}_3\text{MoO}_7$  compound is a semiconductor with a band gap of about 2 eV.

© 2009 Elsevier Inc. All rights reserved.

## 1. Introduction

Compounds of general formula  $\text{Ln}_3\text{MO}_7$ , in which  $\text{Ln}$  is a lanthanide and  $M$  is a pentavalent metal cation, first reported by Allpress and Rossell in 1979 [1], and described as having an orthorhombic, fluorite-related structure with cell dimensions  $a \sim 2a_{\text{fluorite}}$ ,  $b \sim c \sim \sqrt{2}a_{\text{fluorite}}$ . Subsequently, many compositions have been prepared and investigated, including  $\text{Ln}_3\text{MO}_7$  ( $\text{Ln} = \text{La}, \text{Pr}, \text{Nd}; M = \text{Nb}, \text{Ta}, \text{Sb}$ ) [2–6],  $\text{Ln}_3\text{RuO}_7$  ( $\text{Ln} = \text{La}, \text{Pr}, \text{Nd}, \text{Sm}, \text{Eu}, \text{Gd}, \text{Tb}, \text{Dy}$ ) [7–19],  $\text{Ln}_3\text{ReO}_7$  ( $\text{Ln} = \text{La}, \text{Pr}, \text{Nd}, \text{Sm}, \text{Gd}, \text{Tb}, \text{Dy}$ ) [20–23],  $\text{Ln}_3\text{OsO}_7$  ( $\text{Ln} = \text{La}, \text{Pr}, \text{Nd}, \text{Sm}$ ) [24–26], and  $\text{Ln}_3\text{IrO}_7$  ( $\text{Ln} = \text{Pr}, \text{Nd}, \text{Sm}, \text{Eu}$ ) [27–29]. This interest is mostly due to the unusual isolated one-dimensional chains formed by corner sharing  $\text{MO}_6$  octahedra, which are present in these structures. Depending on the electronic configuration of the corresponding transition metal  $M$ , the resulting materials show some interesting electronic and magnetic properties. For example, when the  $M^{5+}$  cation is Nb, Ta, or Sb, the corresponding oxides are electronically inert. When the 5+ metal cation has a  $d$ -electron configuration ranging from  $d^1$  to  $d^4$  ( $M^{5+} = \text{Mo}, \text{Re}, \text{Ru}, \text{Ir}$ ), the  $\text{Ln}_3\text{MO}_7$  compounds are electronically and magnetically active. The magnetic properties of these compounds could be also modulated as a function of the electronic configuration of the  $\text{Ln}^{3+}$  ions. If they contain paramagnetic lanthanides, these contribute to the overall magnetic

properties and can interact with the magnetic moments of the  $M^{5+}$  cations. Another interesting feature of the  $\text{Ln}_3\text{MO}_7$  compounds is the variety of space groups, such as  $Pnma$ ,  $Cmcm$ ,  $C222_1$  or  $P2_12_12_1$ , in which they crystallize. Analogous rare-earth molybdates were first reported by Prévost-Czeskleba in 1987 [30] for  $\text{Ln} = \text{La}, \text{Pr}, \text{Nd}, \text{Sm}, \text{and Eu}$ . Her work on powder samples shows that the latter compounds crystallize in the space group  $Cmcm$ . Later, we obtained single crystals of La, Pr and Sm members [31–33] and showed that these compounds crystallize in the noncentrosymmetric space group  $P2_12_12_1$  at room temperature. We also studied physical properties of  $\text{La}_3\text{MoO}_7$ . Resistivity data showed semiconducting behavior in the range 140–298 K with an activation energy of 0.16 eV. The magnetic susceptibility was quite complex with a broad maximum at 655 K which was interpreted as due to intrachain spin correlations of the  $\text{Mo}^{5+}$  ions. Several other anomalies were observed at 483, 140, and 100 K. More recently, Nishimine et al. [34] reported susceptibility and specific heat measurements on the other members of the  $\text{Ln}_3\text{MO}_7$  series.  $\text{Nd}_3\text{MoO}_7$  shows a clear antiferromagnetic transition at 2.5 K.  $\text{Pr}_3\text{MoO}_7$  and  $\text{Sm}_3\text{MoO}_7$  indicate the existence of magnetic anomaly at 8.0 and 2.5 K, respectively. The DSC measurements indicate that two phase-transitions occur for all  $\text{Ln}_3\text{MO}_7$  compounds in the temperature range between 370 and 710 K.

In this study, we have prepared polycrystalline samples and single crystals of  $\text{Ce}_3\text{MoO}_7$  for the first time. Through single X-ray diffraction measurements, its crystal structure was determined.  $\text{Ce}_3\text{MoO}_7$  has been also characterized through electrical resistivity and magnetic susceptibility measurements.

\* Corresponding author. Fax: +33 2 23 23 67 99.

E-mail address: [patrick.gougeon@univ-rennes1.fr](mailto:patrick.gougeon@univ-rennes1.fr) (P. Gall).

## 2. Experimental

### 2.1. Synthesis and crystal growth

X-ray diffractometrically pure powder of  $\text{Ce}_3\text{MoO}_7$  was prepared from stoichiometric mixtures of  $\text{CeO}_2$  (Rhône-Poulenc, 99.999%),  $\text{MoO}_3$  (Strem Chemicals, 99.9%) and Mo (Cime Bocuze, 99.99%). Before use the Mo powder was heated under a hydrogen flow at 1000 °C for 6 h and the rare earth oxides were pre-fired at 800 °C overnight and left at 600 °C before weighing them. The mixtures were pressed into pellets (ca. 5 g) and loaded into molybdenum crucibles which were previously outgassed at about 1500 °C for 15 min under a dynamic vacuum of about  $10^{-5}$  Torr. The Mo crucibles were subsequently sealed under a low argon pressure using an arc-welding system. The samples were heated at a rate of 300 °C/h to 1400 °C, kept at the temperature for 48 h and then cooled at 100 °C/h down to 1100 °C at which point the furnace was shut down and allowed to cool to room temperature. The resulting product was found to be single-phase on the basis of its X-ray powder diffraction pattern carried out on an Inel position sensitive detector with a  $0^\circ$ – $120^\circ$   $2\theta$  aperture and  $\text{CuK}\alpha_1$  radiation (Fig. 1). Crystals were grown by heating a stoichiometric mixture of rare earth oxide, molybdenum trioxide and molybdenum, all in powder form, in a sealed molybdenum crucible at about 1700 °C for 10 min. The crucible was then cooled at a rate of 100 °C/h down to 1000 °C, and finally furnace-cooled to room temperature. Crystals thus obtained have the shape of needles with quasi-rectangular cross section.

### 2.2. Single crystal X-ray study

The X-ray diffraction data were collected on a Nonius Kappa CCD diffractometer using graphite-monochromated  $\text{MoK}\alpha$  radiation ( $\lambda = 0.71073 \text{ \AA}$ ) at room temperature. The COLLECT program package [35] was employed to establish the angular scan conditions ( $\varphi$  and  $\omega$  scans) used in the data collection. The data set was processed using EvalCCD [36] for the integration procedure. An absorption correction was applied using the description of the crystal faces and the analytical method described by de Meulenaar and Tompa [37]. Analysis of the data revealed that the systematic absences ( $h00$ )  $h = 2n+1$ , ( $0k0$ )  $k = 2n+1$ , and ( $00l$ )  $l = 2n+1$  were consistent with the acentric

orthorhombic space group  $P2_12_12_1$ . The structure was solved with the direct methods program SIR97 [38] and refined using SHELXL97 [39] in the  $P2_12_12_1$  space group. An attempt to refine the structure in the space group  $Pnmm$ , as suggested by the program PLATON [40], was unsuccessful and led to an R factor of about 0.12. The Flack parameter [41] refined to 0.49(6), indicating that the crystal contained a mixture of the two absolute structures. Crystallographic data and X-ray structural analysis for the  $\text{Ce}_3\text{MoO}_7$  compound are summarized in Table 1, and selected interatomic distances are listed in Table 2. Further details of the crystal structure investigation can be obtained from the Fachinformationszentrum Karlsruhe, 76344 Eggenstein-Leopoldshafen, Germany (fax: +49 7247 808 666; e-mail: crysdata@fiz.karlsruhe.de) on quoting the depository number CSD-419443.

### 2.3. Electrical resistivity measurements

The study of the temperature dependence of the electrical resistivity was carried out on a single crystal of  $\text{Ce}_3\text{MoO}_7$  using a conventional ac four-probe method with a current amplitude of 0.1 mA. Contacts were ultrasonically made with molten indium on the single crystal previously characterized on a CAD-4 diffractometer. The ohmic behavior and the invariance of the phase were checked during the different measurements at low and room temperature.

**Table 1**

Crystal data and structure refinements of  $\text{Ce}_3\text{MoO}_7$ .

Empirical formula	$\text{Ce}_3\text{MoO}_7$
Formula weight (g/mol)	628.3
Crystal system, space group	Orthorhombic, $P2_12_12_1$
Unit cell dimensions (Å, deg)	$a = 7.5395(2)$ , $b = 7.6769(1)$ , $c = 10.9769(2)$
Volume (Å <sup>3</sup> )	635.34(2)
Z, calculated density (g/cm <sup>3</sup> )	4, 6.569
Absorption coefficient (mm <sup>-1</sup> )	22.997
Crystal color and habit	Black, needle like
Crystal size (mm <sup>3</sup> )	$0.152 \times 0.063 \times 0.057$
Theta range for data collection (deg)	3.71–39.91
Limiting indices	$-12 \leq h \leq 13$ , $-13 \leq k \leq 13$ , $-19 \leq l \leq 19$
Reflections collected/unique	19818/3903
R (int)	0.0444
Absorption correction	Analytical
Max./min. transmission	0.4142/0.1328
Data/restraints/parameters	3903/0/101
Goodness-of-fit on $F^2$	1.081
R indices [ $I > 2\sigma(I)$ ]	$R1 = 0.0281$ , $wR2 = 0.0473$
Extinction coefficient	0.00418(11)
Largest diff. peak and hole (eÅ <sup>-3</sup> )	2.692 and $-3.235$

**Table 2**

Selected interatomic distances for  $\text{Ce}_3\text{MoO}_7$ .

Mo1–O2	1.865(5)	Ce2–O7	2.313(3)
Mo1–O6	1.916(6)	Ce2–O7	2.361(3)
Mo1–O5	1.979(4)	Ce2–O1	2.421(4)
Mo1–O5	2.007(4)	Ce2–O4	2.429(5)
Mo1–O1	2.030(5)	Ce2–O6	2.548(5)
Mo1–O4	2.051(6)	Ce2–O2	2.560(5)
Ce1–O7	2.401(6)	Ce2–O5	2.664(3)
Ce1–O7	2.407(6)	Ce3–O3	2.306(6)
Ce1–O3	2.415(6)	Ce3–O3	2.312(3)
Ce1–O3	2.416(6)	Ce3–O4	2.453(5)
Ce1–O4	2.550(6)	Ce3–O1	2.474(5)
Ce1–O1	2.639(6)	Ce3–O6	2.508(5)
Ce1–O6	2.822(7)	Ce3–O2	2.531(5)
Ce1–O2	3.096(6)	Ce3–O5	2.603(3)

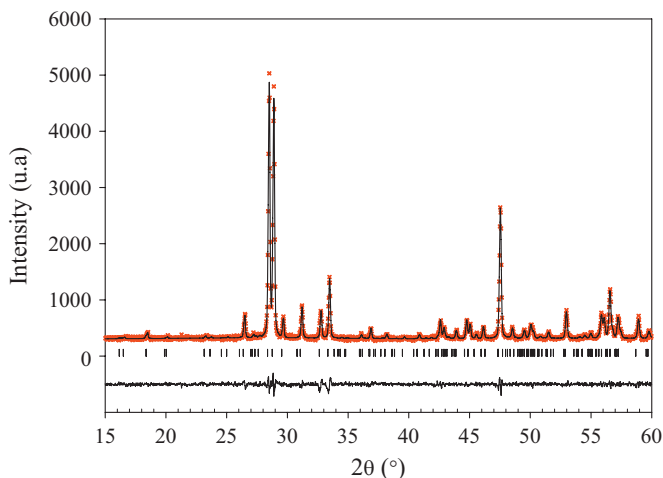


**Fig. 1.** Observed (red crosses), calculated (black continuous line) and difference profiles for the refinement of  $\text{Ce}_3\text{MoO}_7$  in profile-matching mode ( $\lambda = 1.5406 \text{ \AA}$ ). (For interpretation of the references to color in this figure legend, the reader is referred to the web version of this article.)

## 2.4. Magnetic susceptibility measurements

Susceptibility data were collected on cold pressed powder samples (ca. 100 mg) using a Quantum Design SQUID magnetometer between 4.2 and 400 K and at an applied field of 0.1 T.

## 3. Results and discussion

### 3.1. Crystal structure

Fig. 2 shows the variation of the lattice parameters and volume of the  $Ln_3MoO_7$  compounds with the rare-earth size. The  $Ln^{3+}$  ionic radii correspond to a seven coordination and were taken from Ref. [42]. A nearly decrease in all lattice parameters and volume of the orthorhombic unit cells is observed as one moves through the series from the La to the Sm compound. These trends reflect the well-known lanthanide contraction and indicate that all rare earths are trivalent.

Perspective views of  $Ce_3MoO_7$  along the  $b$  and  $c$  axes are shown in (Figs. 3 and 4), respectively. The main structural feature of  $Ce_3MoO_7$  is the occurrence of infinite single chains of tilted corner-linked  $MoO_6$  octahedra running parallel to the  $b$ -axis. These chains alternate with rows of edge-shared  $Ce1O_8$  pseudocubes to form slabs parallel to the  $ab$ -plane. The slabs are separated by the Ce2 and Ce3 cations, which are both seven-coordinated by O atoms forming distorted pentagonal bipyramids.

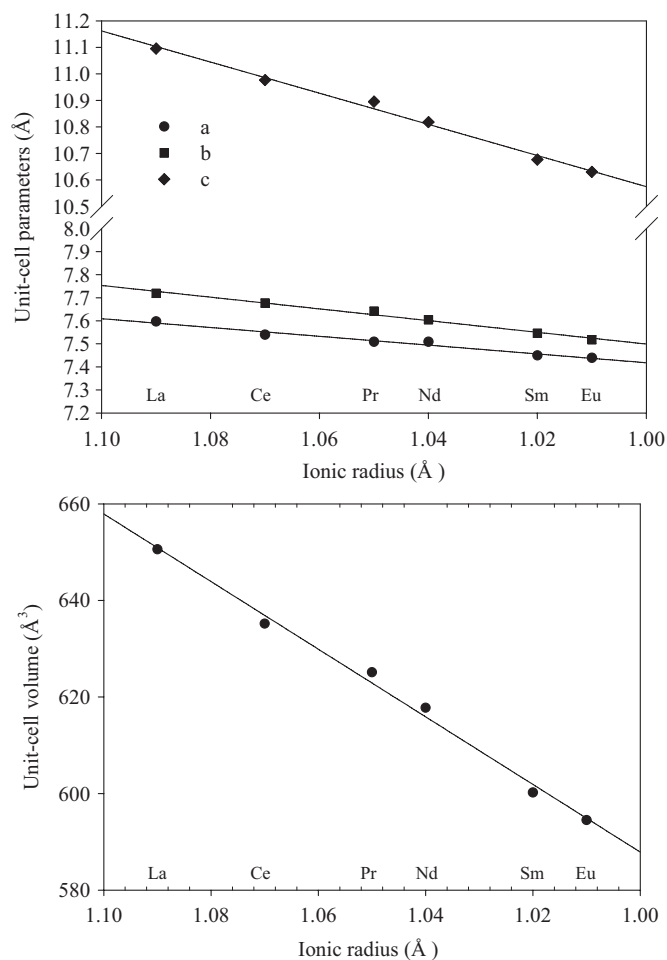


Fig. 2. Variation of the lattice parameters for  $Ln_3MoO_7$  ( $Ln = La$  to  $Eu$ ) as a function of the  $Ln^{3+}$  ionic radius in seven coordination.

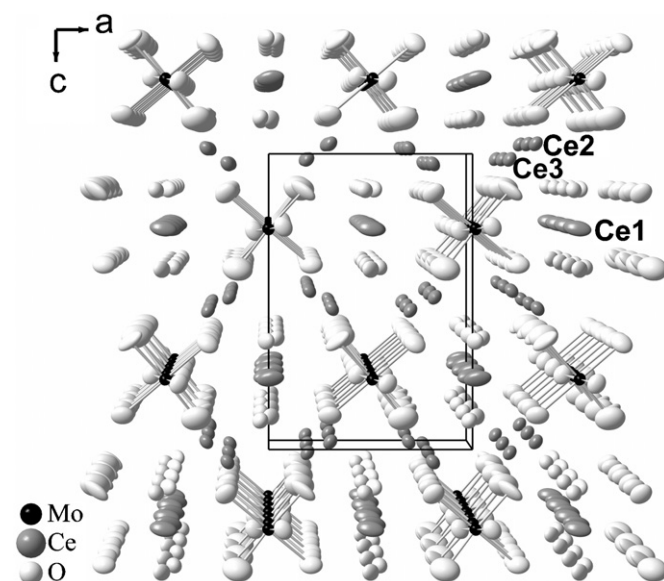


Fig. 3. The crystal structure of  $Ce_3MoO_7$  as viewed down the  $b$ -axis, parallel to the direction of the  $MoO_6$  chain growth. Ellipsoids are drawn at the 97% probability level.

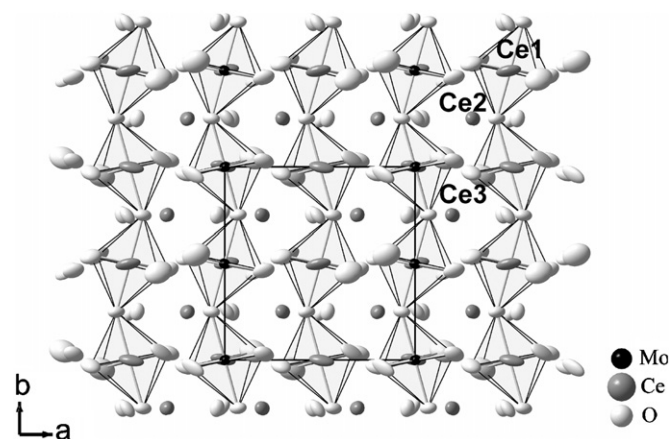


Fig. 4. The crystal structure of  $Ce_3MoO_7$  as viewed down the  $c$ -axis (ellipsoids at the 97% probability level).

The Mo–O distances within the  $MoO_6$  octahedra (Fig. 5) range from 1.865(5) to 2.051(6) Å (1.861(3)–2.098(4), 1.854(4)–2.088(5) and 1.851(3) to 2.088(3) Å in  $La_3MoO_7$ ,  $Pr_3MoO_7$  and  $Sm_3MoO_7$ , respectively, with an average value of 1.975 Å compared with 1.981, 1.974 and 1.966 Å in  $La_3MoO_7$ ,  $Pr_3MoO_7$ , and  $Sm_3MoO_7$ , respectively). Because of the octahedral tilt, the Mo–O5–Mo angle along the chain differs significantly from 180°, with a value of 148.70(15)° in  $Ce_3MoO_7$  (149.1(2)°, 148.3(2)° and 146.62(14)° in  $La_3MoO_7$ ,  $Pr_3MoO_7$ , and  $Sm_3MoO_7$ , respectively). A slight decrease in the Mo–O5–Mo angle is thus observed when the  $Ln^{3+}$  ionic radius also decreases. Deviation from the 180° angle results in a decreased overlap between Mo  $d$  and oxygen  $p$  orbitals, and thus in a tendency for electron localization as reflected by the semi-conducting behavior of the  $Ln_3MoO_7$  compounds. The cerium atoms are located between the  $MoO_6$  chains and occupy three crystallographically inequivalent positions (Fig. 5). The first, Ce1, occupy a pseudo-cubic site with six Ce1–O distances ranging from 2.401(6) to 2.639 (6) Å and two long ones at 2.882(7) and 3.096(6) Å involving the O6 and O2 atoms, respectively. The atoms Ce2 and Ce3 are each coordinated by seven oxygen atoms

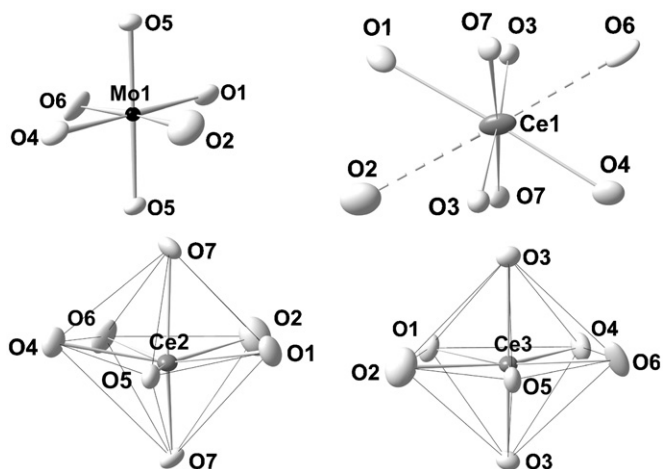


Fig. 5. Oxygen environments for the Mo and Ce atoms (ellipsoids at the 97% probability level).

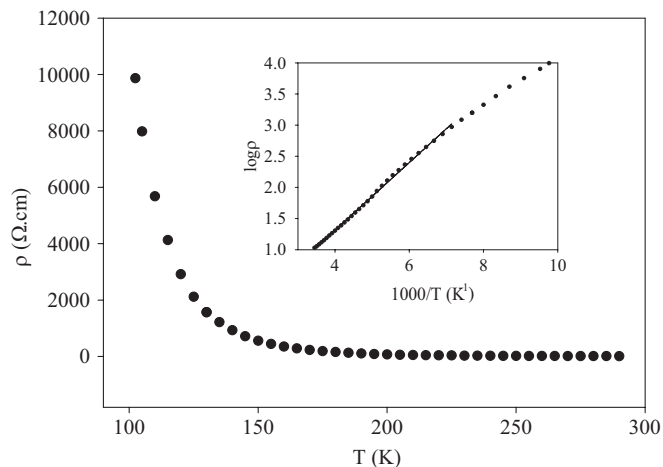


Fig. 6. Temperature dependence of the resistivity for  $\text{Ce}_3\text{MoO}_7$ . The insert shows the Arrhenius plots.

forming a distorted pentagonal bipyramid. For the Ce2 and Ce3 sites, the Ce–O distances spread over smaller ranges, 2.313(3)–2.664(3) and 2.306(3)–2.603(3) Å, respectively. The average Ce–O distances are 2.521, 2.471 and 2.455 Å, for the Ce1, Ce2 and Ce3 sites, respectively. The last two values are very near from that calculated from the sum of the ionic radii, 2.45 Å, while the first one is a little longer.

### 3.2. Electrical and magnetic properties

Electrical resistivity measurements were performed on a single-crystal of the  $\text{Ce}_3\text{MoO}_7$ . The temperature dependence of the electrical resistivity measured along the  $\text{MoO}_6$  chain growth shows that  $\text{Ce}_3\text{MoO}_7$  is semiconducting in the temperature range 100–290 K as shown by the  $\rho$  vs  $T$  and  $\log(\rho)$  vs  $1000/T$  plots (Figs. 6). The room temperature resistivity is about  $10 \Omega\text{cm}$  and the calculated activation energy is 0.21 eV. These values are close to those reported for the  $\text{La}_3\text{MoO}_7$  compound for which the room temperature resistivity is  $11 \Omega\text{cm}$  and the band gap of about 0.16 eV are observed. It is interesting to note that a band gap of 0.28 eV and a room resistivity of  $425 \Omega\text{cm}$  was observed on a polycrystalline pellet of  $\text{La}_3\text{RuO}_7$  [9].

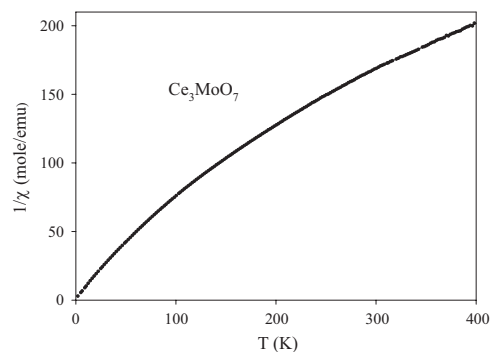


Fig. 7. Reciprocal susceptibility of  $\text{Ce}_3\text{MoO}_7$  as a function of temperature. Data were taken under an applied field of 0.1 T. The solid line represents the fit to a modified Curie–Weiss law in the range of 300–400 K.

The variation of the inverse susceptibility as a function of the temperature for  $\text{Ce}_3\text{MoO}_7$  is displayed in Fig. 7. The high-temperature part of the  $1/\chi$  vs  $T$  plot (data above 300 K) are almost linear. An evaluation of the data for the cerium compound according to a modified Curie–Weiss expression  $\chi = C/(T-\Theta) + \chi_0$  resulted in an experimental magnetic moment of  $2.49 \mu\text{B}$  per cerium atom after subtraction of the magnetic contribution of the  $\text{Mo}^{5+}$  ion, a temperature-independent contribution  $\chi_0 = 5.84 \times 10^{-4} \text{emu/mol}$ , and a paramagnetic Curie temperature (Weiss constant) of  $\Theta = -155 \text{K}$ . The experimental magnetic moment is slightly smaller than the  $\mu_{\text{eff}}$  value of  $2.54 \mu\text{B}$  expected for the free  $\text{Ce}^{3+}$  ion [43]. The plot shows significant deviations from Curie–Weiss behavior below 300 K, most likely due to crystal field splitting of the  $^2F_{5/2}$  ground state of  $\text{Ce}^{3+}$ . No magnetic ordering was evident down to 2 K.

### References

- [1] J.G. Allpress, H.J. Rossell, *J. Solid State Chem.* 27 (1979) 105.
- [2] H.J. Rossell, *J. Solid State Chem.* 27 (1979) 287.
- [3] H.J. Rossell, *J. Solid State Chem.* 27 (1979) 115.
- [4] J.F. Vente, R.B. Helmholdt, D.J.W. Ijdo, *J. Solid State Chem.* 108 (1994) 18.
- [5] A. Kahn-Harari, L. Mazerolles, D. Michel, F. Robert, *J. Solid State Chem.* 116 (1995) 103.
- [6] T. Tanaka, N. Ishizawa, M. Yoshimura, F. Marumo, H. Oyanagi, *J. Solid State Chem.* 114 (1995) 79.
- [7] M. Wakeshima, H. Nishimine, Y. Hinatsu, *J. Phys.: Condens. Matter.* 16 (2004) 4103.
- [8] W.A. Groen, F.P.F. van Berkel, D.J.W. Ijdo, *Acta Crystallogr. C Cryst. Struct. Commun.* 43 (1987) 2262.
- [9] P. Khalifah, R.W. Erwin, J.W. Lynn, Q. Huang, B. Batlogg, R.J. Cava, *Phys. Rev. B Condens. Matter Phys.* 60 (1999) 9573.
- [10] P. Khalifah, Q. Huang, J.W. Lynn, R.W. Erwin, R.J. Cava, *Mater. Res. Bull.* 35 (2000) 1.
- [11] F. Wiss, N.P. Raju, A.S. Wills, J.E. Greedan, *Int. J. Inorg. Mater.* 2 (2000) 53.
- [12] R.P. Bontchev, A.J. Jacobson, M.M. Gospodinov, V. Skumryev, V.N. Popov, B. Lorenz, R.L. Meng, A.P. Litvinchuk, M.N. Iliev, *Phys. Rev. B Condens. Matter Phys.* 62 (2000) 12235.
- [13] D. Harada, Y. Hinatsu, Y. Ishii, *J. Phys.: Condens. Matter* 13 (2001) 10825.
- [14] D. Harada, Y. Hinatsu, *J. Solid State Chem.* 158 (2001) 245.
- [15] D. Harada, Y. Hinatsu, *J. Solid State Chem.* 164 (2002) 163.
- [16] W.R. Gemmill, M.D. Smith, H.C. zur Loye, *Inorg. Chem.* 43 (2004) 4254.
- [17] N. Ishizawa, K. Hiraga, D. du Boulay, H. Hibino, T. Ida, S. Oishi, *Acta Crystallogr. E* 62 (2006) 113.
- [18] N. Ishizawa, T. Suwa, K. Tateishi, *Acta Crystallogr. E* 63 (2007) i163.
- [19] N. Ishizawa, T. Suwa, K. Tateishi, J.R. Hester, *Acta Crystallogr. C* 63 (2007) i43.
- [20] R. Lam, T. Langet, J.E. Greedan, *J. Solid State Chem.* 171 (2003) 317.
- [21] G. Wltschek, H. Paulus, I. Svoboda, H. Ehrenberg, H.J. Fuess, *J. Solid State Chem.* 125 (1996) 1.
- [22] Y. Hinatsu, M. Wakeshima, N. Kawabuchi, N. Taira, *J. Alloys Compds.* 374 (2004) 79.
- [23] M. Wakeshima, Y. Hinatsu, *J. Solid State Chem.* 179 (2006) 3575.
- [24] J.R. Plaisier, R.J. Drost, D.J.W. Ijdo, *J. Solid State Chem.* 169 (2002) 189.
- [25] R. Lam, F. Wiss, J.E. Greedan, *J. Solid State Chem.* 167 (2002) 182.

- [26] W.R. Gemmill, M.D. Smith, Y.A. Mozharivsky, G.J. Miller, H.C. zur Loye, *Inorg. Chem.* 44 (2005) 7047.
- [27] F.P.F. Van Berkel, D.J.W. Ijdo, *Mater. Res. Bull.* 21 (1986) 1103.
- [28] J.F. Vente, D.J.W. Ijdo, *Mater. Res. Bull.* 26 (1991) 1255.
- [29] H. Nishimine, M. Wakeshima, Y. Hinatsu, *J. Solid State Chem.* 177 (2004) 739.
- [30] H. Prévost-Czeskleba, *J. Less-Common Met.* 127 (1987) 117.
- [31] J.E. Greedan, N.P. Raju, A. Wegner, P. Gougeon, J. Padiou, *J. Solid State Chem.* 129 (1997) 320.
- [32] N. Barrier, P. Gougeon, *Acta Crystallogr. E Struct. Rep. Online* 59 (2003) i22.
- [33] N. Barrier, P. Gall, P. Gougeon, *Acta Crystallogr. C: Cryst. Struct. Commun.* 63 (2007) i102.
- [34] H. Nishimine, M. Wakeshima, Y. Hinatsu, *J. Solid State Chem.* 178 (2005) 1221.
- [35] Nonius BV, COLLECT, Data Collection Software, Nonius BV, 1999.
- [36] A.J.M. Duisenberg, *Reflections on area detectors*, Ph.D. Thesis, Utrecht, 1998.
- [37] J. de Meulenaar, H. Tompa, *Acta Crystallogr. A Found. Crystallogr.* 19 (1965) 1014.
- [38] A. Altomare, M.C. Burla, M. Camalli, G.L. Cascarano, C. Giacovazzo, A. Guagliardi, A.G.G. Moliterni, G. Polidori, R. Spagna, *J. Appl. Crystallogr.* 32 (1999) 115.
- [39] G.M. Sheldrick, SHELXL97, Program for the Refinement of Crystal Structures, University of Göttingen, Germany, 1997.
- [40] A.L. Spek, *J. Appl. Crystallogr.* 36 (2003) 7.
- [41] H.D. Flack, *Acta Crystallogr. A Found. Crystallogr.* 39 (1983) 876.
- [42] Y.Q. Jia, *J. Solid State Chem.* 95 (1991) 184.
- [43] J.H. Van Vleck, *Electric and Magnetic Susceptibilities*, Oxford University Press, New York, 1932, p. 243.